

Optimal Friction Materials of Tiny Piezoelectric Ultrasonic Linear Motor

Kyong-Jae Lee and Sahn Nahm

*Department of Materials Science and Engineering, Korea University,
Anam-dong 5-ga, Seongbuk-gu, Seoul 136-701, Korea*

Jin Kyu Kang

*Department of Electrical Engineering, Daelim College,
Bisan 1-dong, Dongan-gu, Anyang-si, Gyeonggi 431-715, Korea*

Hyun-Phill Ko, Chong-Yun Kang, Hyun-Jae Kim, and Seok-Jin Yoon^a

*Thin Film Materials Research Center, Korea Institute of Science and Technology(KIST),
Hawolgok 2-dong, Seongbuk-gu, Seoul 136-791, Korea*

^aE-mail : sjyoon@kist.re.kr

(Received August 22 2005, Accepted December 6 2005)

In recent years, a novel tiny piezoelectric linear motor converting a radial mode vibration to a longitudinal mode vibration driven by the impact force has been developed for a camera optical module. The tiny piezoelectric motor is consisted of a shaft, mobile element, and piezoelectric transducer. In this work, the frictional coefficient and static friction force of the interface between the shaft and the mobile element have been investigated according to their respective materials. It was found that two combinations, namely Pyrex glass or stainless steel for the shaft and stainless steel (SUS) for the mobile element, exhibited good dynamic behaviors in the tiny ultrasonic linear motor, which was newly developed based on operating concepts based on Newton's law.

Keywords : Piezoelectrics, Linear motor, Friction coefficient, Transducer, Shaft, Mobile

1. INTRODUCTION

Many types of ultrasonic motors which are operated on principles entirely different from those known thus far have been developed since the first piezoelectric ultrasonic motor was developed in 1970s by H. V. Barth[1] and V. V. Lavrinenco[2]. In recent studies, a tiny ultrasonic linear motor which changes the vibration direction by piezoelectric ceramics has been introduced[3-6]. The driving force of ultrasonic motors is generated by piezoelectrically excited ultrasonic vibration and friction force, which differs significantly from electromagnetic motors that utilize the Lorentz force. In general, the ultrasonic motor's features are mentioned such as a high torque at a comparatively low speed of rotation, small volume with no gears, low energy consumption and no electromagnetic noise due to the absence of coil and magnetic material.

Several decades have passed since the development of ultrasonic motors and some instances of their

implementation are found[7-8], however the stage of their wide application has not been reached. Their characteristics, particularly the driving and control techniques, are completely different and their applications are not established. Since the driving force is transferred by friction on the contact surface, investigating the frictional properties take on an important role for improving the movement characteristic of a motor.

In this study the frictional properties between the shaft materials and the mobile materials were intensively considered by changing the materials which have different coefficient of friction, and the optimal combinations of material for shaft and mobile were recommended.

2. EXPERIMENTS

2.1 Material preparation

In order to investigate the frictional properties of the

Table 1. Physical properties of Bakelite and Stainless steel substrate.

Classification(μm)	Bakelite	Stainless steel
Roughness(μm)	Ra(L)=0.33~1.0 μm	Class 1 : 0.017 μm
	Ra(T)=0.49~3.4 μm	Class 2 : 0.026 μm
		Class 3 : 0.038 μm
Hardness(Hv)	24	220

interface between the shaft and mobile element according to their respective materials, four types of materials were used for the shaft, i.e., the stainless steel balls coated with DLC(Diamond-like carbon) and PTFE (Polytetrafluoroethylene), the uncoated stainless steel balls(AISI52100), and Pyrex glass balls(SiLibeads) with diameters of 6 mm. The stainless steel balls were coated with DLC film with a thickness of 4 μm by radio-frequency plasma-assisted chemical vapor deposition(rf PACVD) and PTFE film with a thickness of approximately 10~15 μm by the spray coating method. The frictional coefficient between the steel balls and the DLC film is generally in the range of 0.1 to 0.4 in an ambient environment, but is as low as 0.02 in a dry atmosphere or high vacuum[9-11]. Because DLC films exhibit very low friction and high wear resistance, they can be used as solid lubricating materials in the field of engineering. PTFE is another important engineering material, since it exhibits a low coefficient of friction when rubbed against metallic engineering surfaces. However, the wear resistance of PTFE is rather low, which somewhat impairs its usefulness as an engineering material[12]. In the case of stainless steel and Pyrex glass, the frictional coefficient is generally very high (about 0.6~0.7) in low relative humidity air.

For the substrate materials, bakelite and stainless steel substrate with a diameter of 30 mm and a thickness of 5 mm were used. The cotton fibers of 125 μm in thickness were embedded in the bakelite, and stainless steel is classified into three classes, 1, 2, and 3, according to the roughness average(Ra). Table 1 shows the physical data concerning the substrate materials, where Ra(L) and Ra(T) mean that the roughness average is measured parallel and perpendicular to the fiber, respectively.

2.2 Experimental method

In this work, two testing systems were used to determine the optimal frictional materials for the shaft and mobile element, by measuring the frictional properties. One is the ball on a disc type tribometer, which is used for characterizing the coefficient of friction of the two types of material, and the other is a universal test machine (Instron4464, INSTRON Co.) which is used to determine the maximum static friction force.

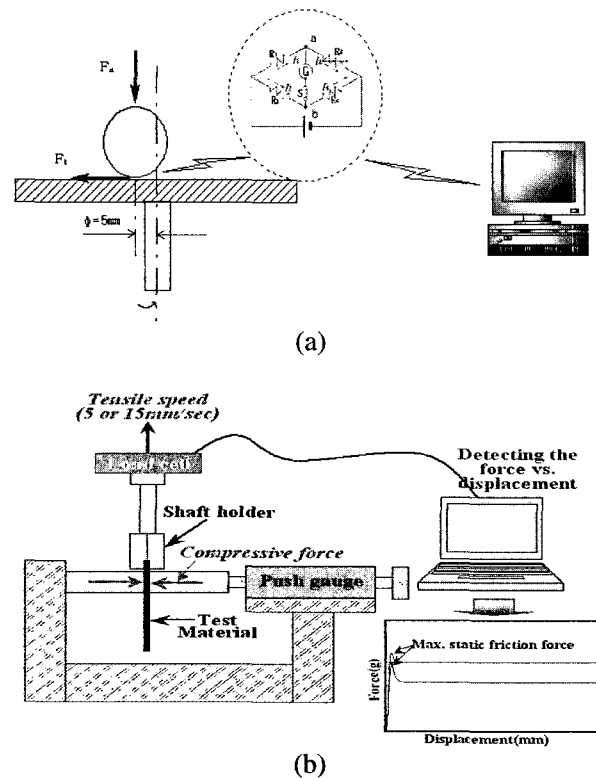


Fig. 1. Schematic diagram (a)tribometer (b)universal test machine(UTM).

Table 2. Roughness of the shafts.

Classification	Stainless steel	DLC coated	Pyrex	PTFE coated
Ra(μm)	0.19	0.22	0.09	1.45

Figure 1 shows a schematic diagram of the tribometer and the universal testing machine. The frictional test was performed in ambient air condition using the tribometer shown in Fig. 1(a). The temperature and the relative humidity were in the range from 20 to 25 $^{\circ}\text{C}$ and from 15 to 30 %, respectively. The balls with a diameter of 6mm slid over the surface of the bakelite and stainless steel substrates, which had a diameter of 30 mm and a thickness of 5 mm. The samples were placed on a

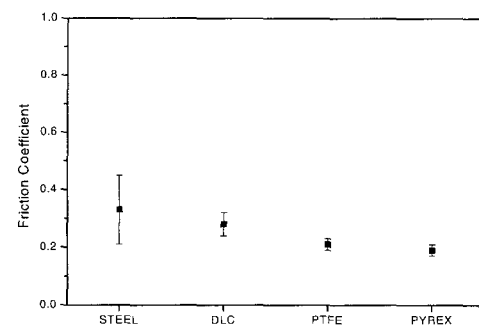
specimen holder that was installed on the rotating axis of an AC servo motor. The rotation speed and normal load were fixed at 220 rev min^{-1} (11.5 cm s^{-1}) and 2 N. The maximum number of contact cycles was 13,000.

In order to investigate the maximum static friction force, four kinds of shafts, 0.8~1.0 mm in diameter and 10~14 mm in height, were prepared using different surface materials such as DLC and PTFE coated stainless steel shafts, uncoated stainless steel shafts, and Pyrex shafts. The maximum static friction force was measured using the universal test machine (Instron 4464) with a 250 g load cell at different tensile speeds (5 mm/sec and 15 mm/sec). When the shaft was pulled upward, a compressive force of 0.2 N, 0.6 N and 1.0 N was applied by the holder, which was made of either bakelite or stainless steel. Table 2 shows the roughness average of the shaft materials.

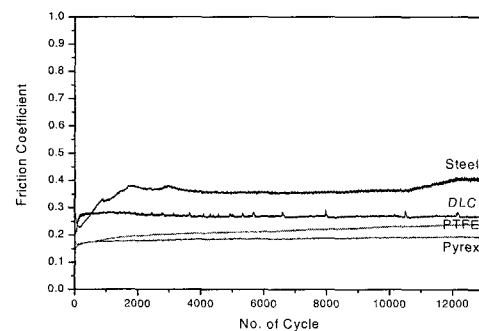
3. RESULTS AND DISCUSSION

Figure 2 shows the frictional properties of DLC and PTFE coated stainless steel, uncoated stainless steel, and Pyrex ball against the bakelite substrate. The frictional coefficients in Fig. 2(a) were obtained by averaging the frictional coefficients after repeating the experiments several times. On the whole, all of the specimens had lower frictional coefficients against the bakelite substrate than against the stainless steel substrate. (see Fig. 3(a)) The range of average frictional coefficients was from 0.19 to 0.33. The frictional coefficient of the uncoated stainless steel ball to bakelite substrate was the highest (about 0.33), while the frictional coefficient of DLC coated ball to bakelite substrate was the lowest (about 0.19). Fig. 2(b) illustrates the frictional behaviors of the samples against bakelite in an air environment. It is obvious that the frictional behavior of steel is very different from that of the other materials. At the beginning of the test (about 0~200 cycles) the frictional coefficient of the stainless steel ball decreases slightly, and then increases in the range of cycles from 200 to 2000. The decline of the coefficient during the first 200 cycles is assumed to result from the very thin oxide layer (\AA order) of the steel ball surface causing the ball to have a low frictional coefficient. After approximately 2000 cycles, the frictional coefficient of steel reaches the steady state. The average coefficients of friction for DLC and PTFE coated ball and Pyrex ball were about 0.28, 0.21 and 0.19, respectively.

Higher coefficients of friction were observed against the stainless steel substrate, as shown in Fig. 3. In Fig. 3(a) the average frictional coefficients of all of the specimens except for DLC were higher than those observed for the bakelite substrate. In particular, the average frictional coefficient of DLC did not vary



(a)

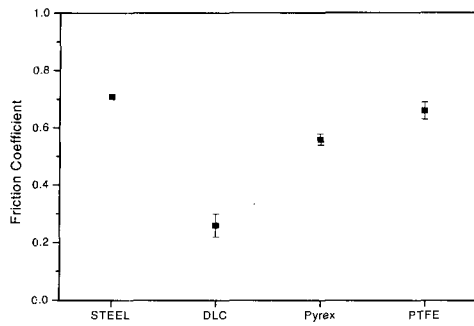


(b)

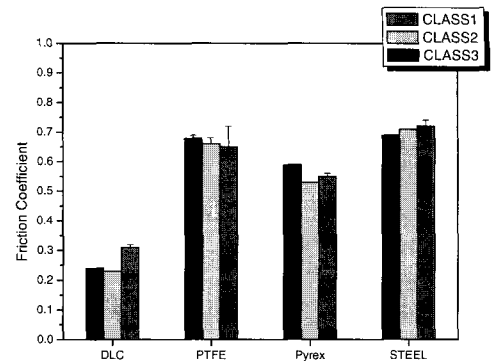
Fig. 2. Variation of the frictional behaviors of uncoated stainless steel ball, DLC and PTFE coated ball, and Pyrex ball on the bakelite substrate (a) average coefficient of friction (b) evolution of the frictional coefficient with increasing number of contact cycle (@Normal load=2 N, 220 rpm, 1 hr).

significantly according to the substrate material. This stability of the frictional behavior of DLC, irrespective of the substrate material, is assumed to be because DLC film has an extreme hardness, a low friction coefficient and high chemical resistance. Also, the coefficient of friction of PTFE is very low, about 0.09, but it has relatively poor wear resistance, because of the extremely high cohesive energy density of the PTFE molecule and the weak intermolecular strength.

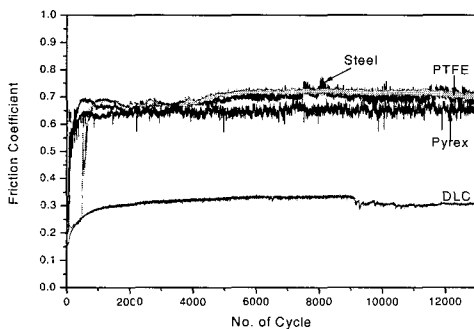
Therefore, PTFE easily shears and yields. As a result, the frictional coefficient and wear resistance of PTFE is generally low. In Fig. 3(b), the coefficient of friction of PTFE remained at a low value (~ 0.22) until about 500 cycles, while above 500 cycles, the frictional coefficient jumped abruptly to 0.65, because the coating layer of PTFE came off, exposing the surface of the stainless steel. The point of about 500 cycles, therefore, can be regarded as the transition region in which the contact surface of the PTFE is changed.



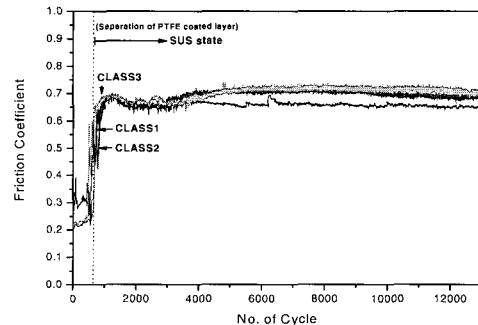
(a)



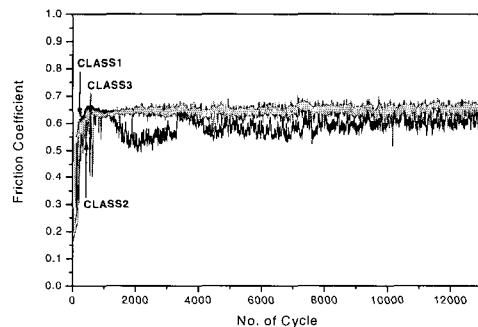
(a)



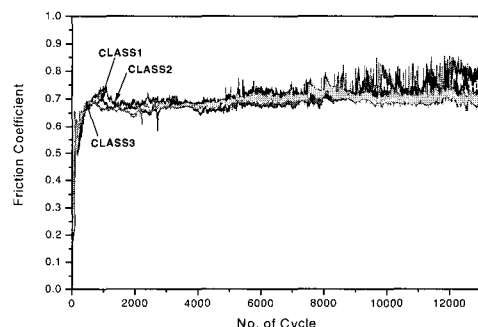
(b)



(b)



(c)

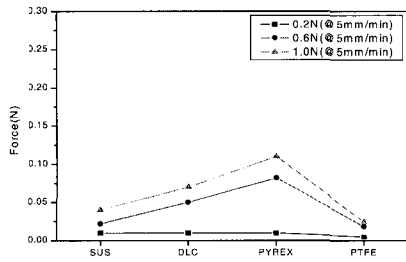


(d)

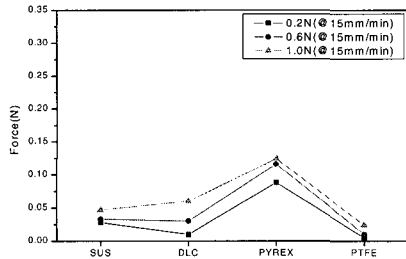
Fig. 3. Variation of the frictional behaviors of Steel, DLC, PTFE and Pyrex ball against the stainless steel substrate (a)average coefficient of friction (b)evolution of the frictional coefficient with increasing number of contact cycle(@Normal load=2 N, 220 rpm, 1 hr).

Figure 4 shows the frictional coefficient characteristics of the balls against the stainless steel substrates according to their surface roughness, i.e., class1, class2 or class3. In Fig. 4(a), it is evident that the frictional coefficients of the PTFE coated ball, Pyrex ball and stainless steel ball show similar values, regardless of the surface roughness of the stainless steel substrate. However, in the case of the DLC group, when the DLC ball and substrate were in contact at the interface, since the smaller surface roughness caused the contact surface to be larger, the class 1(smallest roughness in this experiment) substrate showed a higher coefficient of friction. The evolutions of the frictional behaviors of the specimens are shown in Fig. 4(b), (c), and (d). In particular, the frictional behavior of PTFE coated ball shows the existence of a transition region at around 600 cycles, at which point the contacting surface changed from the PTFE coated ball to the stainless steel ball, because of the detachment of the PTFE coated layer.

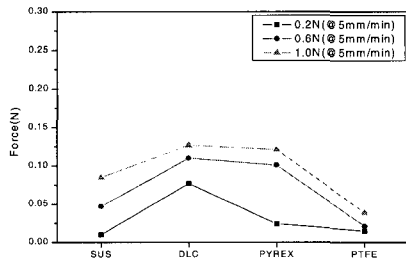
Fig. 4. Frictional coefficient characteristics of stainless steel substrate with various roughness (Ra) (a)average frictional coefficients (b)PTFE coated ball (c)Pyrex ball (d)stainless steel ball(where normal load,2 N; speed, 220 rpm; sliding time,1 hr; Class1,0.017 μm ; Class2,0.026 μm ; Class3,0.038 μm).



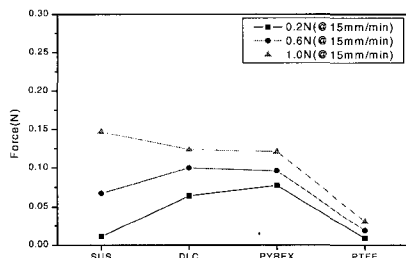
(a)



(b)



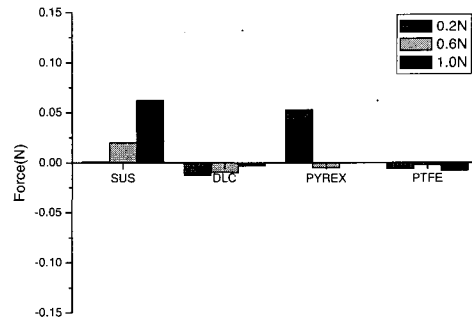
(c)



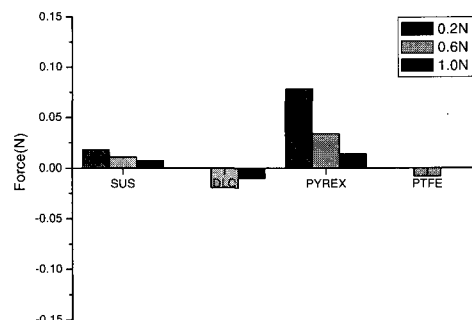
(d)

Fig. 5. Variation of maximum static friction force relative to the 0.2 N, 0.6 N, 1.0 N compressive force at 5 and 15 mm/min;(a),(b) against stainless steel substrate and (c),(d) against bakelite substrate.

Another test was carried out for the purpose of measuring the maximum static friction force of the materials using the universal test machine (UTM, Instron4464). Figure 5 shows the variations in the maximum static friction force when the compressive force was changed from 0.2 N to 1.0 N using the holders made of bakelite and stainless steel materials, and the tensile speed of the shaft was changed from 5 mm/sec to



(a)



(b)

Fig. 6. Changes of maximum static friction force relative to tensile speed (from 5 mm/min to 15 mm/min) at 0.2 N, 0.6 N, 1.0 N (a) bakelite mobile (b) stainless steel mobile.

15 mm/sec. In general, the maximum static friction force increased as the compressive force or tensile speed of the shaft increased.

Figure 6 shows the change in the maximum static friction force when the tensile speed was increased from 5 to 15 mm/sec. In Fig. 6, it can be seen that the maximum static friction force varies with the tensile speed. If the change in the maximum static friction force of the coupling between the shaft and the mobile material in the piezoelectric ultrasonic linear motor system has a negative value, this implies that the mobile material, which is suspended on the shaft by the frictional force generated by the compressive force, slips when the piezoelectric actuator is vibrated by AC voltage at an ultrasonic frequency. Also, this implies that the dynamic properties of the ultrasonic linear motor driven by the frictional force of the shaft and mobile element are not satisfactory.

As a result of our investigation into the changes in the maximum static friction force according to the tensile speed, it is shown in Table 3. that two couplings, (1) SUS mobile/Pyrex (or stainless steel) shaft (2) bakelite mobile/Pyrex shaft, have relatively better properties than those of the other couplings, without any slip of the mobile element.

Table 3. Changes of the maximum static friction force between the shaft and mobile element materials(Tensile speed : 5 mm/sec and 15 mm/sec).

Shaft	SUS material			Bakelite material		
	0.2 N	0.6 N	1.0 N	0.2	0.6 N	1.0 N
DLC coated	*	-	-	-	-	*
Pyrex	+++	+	+	++	-	*
Stainless steel	++	+	+	+	+	+
PTFE coated	*	-	*	-	-	-

+++ : Increase (more than two times), ++ : Increase (about one time), + or - : Increase or decrease (less than one time), * : No change

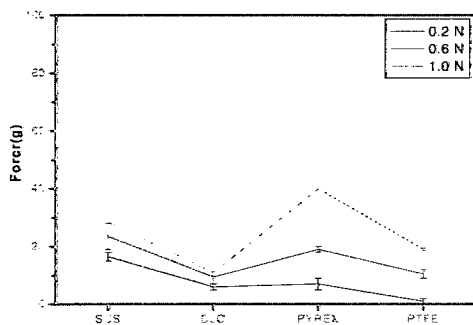


Fig. 7. Thrust force of the linear motor with various shafts in accordance with the compressive force of stainless steel mobile.

Also, when the shafts manufactured with the various materials, i.e., DLC and PTFE coated steel, the uncoated stainless steel and Pyrex glass rod, are compressed by the mobile element made of stainless steel material, the thrust force of the shaft in the ultrasonic linear motor is measured by the force gauge throughout this operation. Figure 7 shows the data for the thrust force of the shafts, which depends on the compressive force applied to the shafts, that is, the larger the compressive force, the higher the thrust force of the shaft in the range of operating frequencies of the ultrasonic linear motor. In particular, the Pyrex shaft was sensitively affected by the compressive force, whereas the DLC coated shaft was not, i.e. the shaft made of Pyrex has a large thrust force at a high compressive force, whereas the stainless steel shaft has a large thrust force at a low compressive force. In the case of the bakelite mobile element, none of the shafts had good properties in terms of the thrust force. The qualitative results of this test are shown in Table 4.

Table 4. Qualitative property analysis of the thrust force between the linear motor shaft materials and stainless steel mobile relative to the compressive force (at 0.2 N, 0.6 N, and 1.0 N).

Shaft Materials	Thrust Force (g)		
	0.2 N	0.6 N	1.0 N
DLC coated	△	△	△
Pyrex	○	○	◎
Stainless steel	◎	◎	○
PTFE coated	△	○	○

◎ : Excellent ○ : Good △ : Good or bad (unstable)

4. CONCLUSION

We investigated the frictional coefficient and thrust force between the shaft and mobile materials with two different techniques, namely using a tribometer and a universal test machine (UTM). In this study, shafts made of DLC and PTFE coated stainless steel, the uncoated stainless steel and Pyrex, and the mobile elements made of bakelite and stainless steel, were used. We investigated the changes in the frictional coefficients by means of the frictional test and found that the optimal shaft/mobile couplings were stainless steel shaft/stainless steel mobile and Pyrex shaft / stainless steel mobile in a novel tiny ultrasonic linear motor driven by the new principle and the frictional force between the shaft and the mobile element.

REFERENCES

- [1] H. V. Barth., "Ultrasonic driven motor", IBM Tech, Disclosure Bull., Vol. 16, No. 7, p. 2263, 1973.
- [2] V. V. Lavrinenco, S. S. Vishnevski, and I. K. Kartashev, "Izvestiya Vysshikh Uchebnykh Zavedenii", Radioelektronika, Vol. 13, p. 57, 1976.
- [3] S.-J. Yoon, J.-W. Choi, S.-J. Kim, Y.-T. Yu, and H.-J. Kim, "Design of shaking beam for piezoelectric linear ultrasonic motor", J. of the Korean Ceramic Society, Vol. 40, No. 11, p. 1062, 2003.
- [4] D.-K. Lee, D.-Y. Han, S. Borodinas, P. Vasiljev, and S.-J. Yoon, "Compound linear ultrasonic motor based on shaking beam", Jpn J. Applied Phys., Vol. 43, No. 4A, p. 1454, 2004.
- [5] K. J. Lee, D.-K. Lee, S. Borodinas, P. Vasiljev, S. Nahm, and S.-J. Yoon, "Analysis of shaking beam actuator for piezoelectric linear ultrasonic motor", IEEE Trans. Ultrason., Ferroelect., Freq. Contr., Vol. 51, No. 11, p. 1508, 2004.

- [6] H.-P. Ko, S. S. Kim, C.-Y. Kang, H.-J. Kim, S.-J. Yoon, "Optimization of a piezoelectric linear motor in terms of the contact parameters", *Materials Chemistry and Physics*, Vol. 90, No. 2-3, p. 322, 2005.
- [7] S. Ueha and Y. Tomikawa, "Ultrasonic Motors, Theory and Applications", Oxford University Press, 2005.
- [8] T. Sashida and T. Kenjo, "An Introduction to Ultrasonic Motors", Oxford University Press, 1994.
- [9] K. Enke, "Some new results on the fabrication of and the mechanical, electrical and optical properties of i-carbon layers", *Thin Solid Films*, Vol. 80, No. 1/3, p. 227, 1981.
- [10] R. Memming, H. J. Tolle, and P. E. Wierenga, "Properties of polymeric layers of hydrogenated amorphous carbon produced by a plasma-activated chemical vapour deposition process II: Tribological and mechanical properties", *Thin Solid Films*, Vol. 143, No. 1, p. 31, 1986.
- [11] B. Marchon, N. Heiman, and M. R. Khan, "Evidence for tribochemical wear on amorphous carbon thin films", *IEEE Trans. Magn.* Vol. 26, No. 1, p. 168, 1990.
- [12] S. K. Biswas and K. Vijayan, "Friction and wear of PTFE – a review", *Wear: An international journal on the science and technology of friction, lubrication and wear*, Vol. 158, No. 1/2, p. 193, 1992.